Magnetization step, history-dependence, and possible spin quantum transition in $Pr_{5/8}Ca_{3/8}MnO_3$ manganites

Guixin Cao, Jincang Zhang,* Shixun Cao, Chao Jing, and Xuechu Shen
Department of Physics, Shanghai University, Shanghai 200436, China
(Received 4 August 2004; revised manuscript received 10 November 2004; published 19 May 2005)

In order to clarify the physical mechanism of magnetization step in strong correlation manganites with a phase separation, one $Pr_{5/8}Ca_{3/8}MnO_3$ single crystal was successfully grown by the optical floating-zone method and investigated systematically on its structural, magnetic, and transport properties. One steplike charge ordered antiferromagnetic-ferromagnetic transition was proved below 60 K as an applied magnetic field is only several *T*, and the step in the *M-H* curve became ultrasharp below 4.2 K. A history-dependent magnetization effect was also observed. Here, the given charge/orbital ordering and spin structure indicated that the energy difference between ferromagnetic and charge ordering phases was small for $Pr_{5/8}Ca_{3/8}MnO_3$. According to the model of spin and orbital coupling, the steps should be the result of spin reorientation under the magnetic field. Meanwhile, the two sharp step transitions appeared in the different field-cooled (FC) conditions at $T = 2.0$ K, which shows a possible existence of spin quantum transition. The observed history-dependent magnetization reflected the existence of $d_{x^2-y^2}$ orbital ordering state within the FM state. The correlation between the magnetic structure and the mechanism was also discussed.

DOI: 10.1103/PhysRevB.71.174414 PACS number(s): 75.30.Kz, 71.30.+h, 71.27.+a

I. INTRODUCTION

Perovskite-type manganites with the general chemical formula $R_{1-x}A_xMnO_3$ (*R* and *A* being rare- and alkaline-earth ions, respectively) have been extensively researched because of their rich physical contents by various behaviors of electrical transport and magnetic properties, which would be very important to clarify the physical mechanism of strong correlation electron system and colossal magnetoresistance (CMR) effect.[1,2] The basic microscopic picture responsible for the insulator-metal transition in the manganites has been established, which is believed to be the percolative transport through the coexistence phase of the submicrometer charge-ordered antiferromagnetic-ferromagnetic (COAFM) and FM transitions. The phase separation scenario is intrinsic in these materials and is attracting considerable attention. Nevertheless, the physics of the CMR effect, especially the microscopic mechanism of the correlations among spin, charge, orbital, and lattice degrees of freedom, is far from being completely understood. Recently, several unexpected and intriguing magnetization steps were observed for Mn-site substituted manganese oxides $Pr_{1-x}Ca_xMn_{1-y}M_yO_3$ with $x \sim 0.5$, $y \sim 0.05$ (*M* is Ga, Cr, Sc, and Co, etc.).[3–5] This was thought that the Mn-site substitution weakens the COAFM state and favors the development of PS, then make the required magnetic fields decrease. It is well known that the Mn-site substitution is very efficient in destabilizing the strongly charge and orbital ordering.[6] Nevertheless, there is also the observation of similar steplike transitions in $Pr_{0.7}Ca_{0.3}MnO_3$ and $Sm_{0.5}Sr_{0.5}MnO_3$.[5] In these PS compounds, the magnetic field needed to cause the steps is only several T. Generally, via a traditional metamagnetic transition,[7] it will need very high magnetic fields larger than 20.0 T to overcome this AFM state. Here, the lower critical magnetic field driven the transition shows that this magnetization steps are different from the traditional antiferromagnetic transition. In addition, recent literature proposed that this magnetization transition is related to the martensitic character associated with the strain between the PS regions.[8] In the martensitic model, the COAFM and FM phases are looked upon as a high-temperature-phase (austenite) and a low-temperature-phase (martensite), respectively. The step-type COAFM-FM transition was driven by applied magnetic field when the driving force (i.e., the magnetic energy) overcomes the elastic energy associated with the strains created at the COAFM/FM interfaces. The COAFM phase has significantly larger lattice parameters and unit-cell volume than that of the ferromagnetic phase, and the unit-cell of the antiferromagnetic (AFM) phase is strongly distorted. As a magnetic field is applied in the sample, the strains created in the AFM/FM interfaces tend to block the development of the magnetic energy. And when the applied field is sufficient to overcome the stress energy, the magnetization will appear a sudden increase, which makes this martensitic transformation be discontinuous with burstlike effects. In this model the effect of an external magnetic field would be only to overcome the stress energy and promote the growth of FM phase fraction, without modifying the magnetic coupling of the spins. Though this martensitic scenario is attracting considerable attention, the observation of sharp *M-H* steps in the underdoped $Pr_{0.7}Ca_{0.3}MnO_3$ points towards the role of the OO/CO state,[9] and such a picture did not consider the influence of microstructure on the appearance of *M-H* steps. Moreover, it is difficult to reconcile with some experimental results that the *M-H* step shows a gentle transition when above certain temperature point.[5] In this paper, we show that the *M-H* steps in PCMO are indeed far more complex than the simple martensitic transition due to the sudden growth of FM phase. Instead, our study indicates that the *M-H* steps are associated with the spin reorientation under the magnetic field and there exists a possible spin quantum transition. The result challenges our present understanding the mechanism of the *M*

-*H* steps and suggests that, if martensitic effect plays an important role in the AFM-FM transition process, it must consider the stress would influence the spin and orbital state of the AFM phase fraction and its transformation under field cannot be ignored for the appearance of *M*-*H* steps.

The above features prompted us to undertake a systemic study about this peculiar COAFM-FM transition. In this work, the Mn-doping free $Pr_{5/8}Ca_{3/8}MnO_3$ (PCMO) single crystal was used to study this dreamscape magnetization. Based on its coexistence characteristics of FM, AFM, and CO phase at low temperature, it should be reasonable to predict that the unusual steps in magnetization and related properties might be observed in PCMO as an applied magnetic field change. The structural, magnetic and transport properties of single-crystal PCMO were investigated. The COAFM-FM step transition is found in the *M*-*H* curve below 60 K as the applied magnetic field is only several tesla, and the step becomes ultrasharp below 4.2 K. The two similar sharp step transitions in the different FC conditions and the history-dependent magnetization effects were also observed. This kind of step transition should be the result of spin reorientation under the magnetic field and there exists a possible spin quantum transition. Above 10.0 K, however, the step was not sharp, which was caused by the effect of thermal fluctuations that smears the transition and affects the fluctuation rate of orbital. The related mechanism and possible interpretations were also discussed.

II. EXPERIMENTAL DETAILS

A single crystal of $Pr_{5/8}Ca_{3/8}MnO_3$ (PCMO) with a size of 32 mm in length and 4 mm in diameter was grown by optical floating-zone method in a flowing O_2 atmosphere (100 cc/min) at a rate of 2 mm/h. The rod was cut and two slices were obtained with a size of 0.5 mm thick along longitudinal and transversal section, respectively. Then they were polished for microstructural analysis. X-ray-diffraction measurement revealed a good single-phase structure and showed that the longitudinal section of the slices is in the *a*-*b* plane and the transversal section is along the *c* axis. Low-temperature x-ray-diffraction data for single crystal PCMO were obtained by 18 kW D/max-2550 using Cu-K_α radiation in the range of 300–10 K. Magnetic measurements were carried out using PPMS-9 (physical property measurement system, Q/D Inc., US) with the precision 20 nV for voltage, and 0.2 Oe for the magnetic field. All the *M*-*H* curves were recorded after the sample was cooled under zero-field cooling (ZFC) or field cooling (FC) condition from the paramagnetic state at 300 K. Resistivity measurements were carried out using the conventional four-probe technique. The resistivity vs temperature ρ-*T* curves measured under applied dc magnetic fields ranges from 0–6.0 T were recorded by PPMS in the range of 1.9–300 K with a temperature precision of 0.01 K. The experiment results are repeatable.

III. RESULTS AND DISCUSSION

A. Transport characteristics, structure, and orbital ordering

Figure 1 showed the temperature dependence of resistivity for cooling and heating conditions at the applied magnetic fields of 0.0, 3.0, and 6.0 T, respectively. It can be seen that both the curves under zero field and 3.0 T have a semiconducting behavior and superposed for the same field during cooling and heating. On the other hand, these ρ-*T* curves show a superposition above 230 K and a discernible upturn around 230 K, which corresponds to the onset of CO.[10] According to Asaka's work, the present onset has confirmed the existence of superlattice structure below 230 K for PCMO as a further evidence of the $d_{3x^2-r^2}/d_{3y^2-r^2}$-type charge/orbital ordering by low-temperature transmission electron microscopy.[11] An applied magnetic field of 6.0 T drastically modifies such an insulating CO state and the ρ-*T* curve undergoes a *I*-*M* transition at $T_p \approx 84$ K (peak value) for the cooling curve and $T_p \approx 110$ K for the heating curve. This shows that the transition becomes strongly hysteretic and the first-order transition exists in the present system. However, it must be noted that the low-temperature resistivity below T_p (28 Ohm cm) is larger than the Mott's maximum metallic limit. Figure 2 shows the temperature dependence of the *M*-*T* curve measured on heating for ZFC and FC in a field of 6.0 T. The inset displays resistivity curves recorded under the same conditions. The *M*-*T* curves display the same general features as the similar compounds ($0.3 \leqslant x \leqslant 0.4$):[11,12] (i) two kinks correspond to the CO temperature T_{CO} and Nèel temperature T_N around 230 and 160 K, respectively; (ii) at low temperature, magnetization *M* appears an large increase at about 70 K for the cooling curve and 102 K for the heating curve, respectively. If associating these temperatures with the onset of FM ordering, we can find that the *I*-*M* transition temperature, as shown in Fig. 1 and in the inset of Fig. 2, is higher than T_C, which probably shows that the true T_C in the system is considerably higher than observed in the present experiment. Below about 100 K, the ZFC and FC curves separate from each other when approaching the phase separation region. This feature displays the first order characteristics of this ferromagnetic transition. Meanwhile, it suggests that both magnetization and resistivity are related to dependence on the magnetic history as shown in Sec. III C. This further indicates that it is not induced by the transition

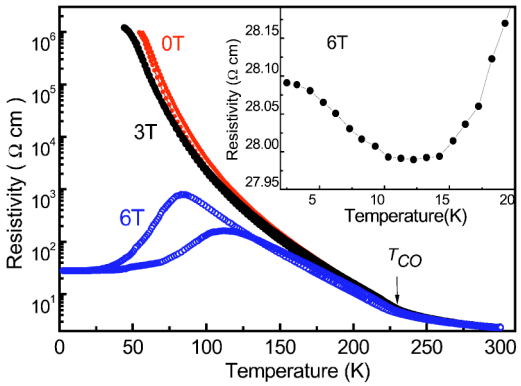

FIG. 1. (Color online) The temperature dependence of resistivity under 0, 3.0, and 6.0 T for $Pr_{5/8}Ca_{3/8}MnO_3$. The resistivity was measured in FC mode. Inset gives the magnified curves of ρ-*T* under 6 T at below 20 K, which shows a distinct minimum in the vicinity of 13 K.

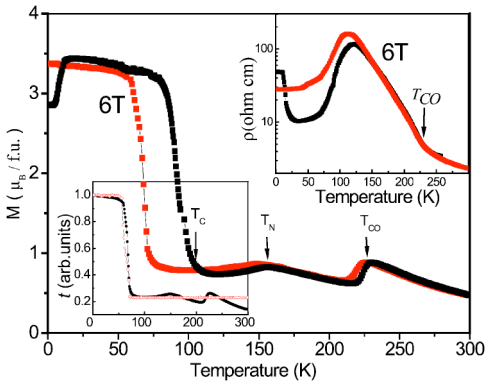

FIG. 2. (Color online) dc magnetization curves of $Pr_{5/8}Ca_{3/8}MnO_3$ in a applied field of 6.0 T. The black and red symbols correspond to the ZFC and FC modes, respectively. Inset in the top right corner displays resistivity curves recorded in the same conditions, and in the down left corner is the transfer amplitude t as a function of temperature (black and red symbols stand for experimental and fitted curves, respectively).

from an orbital ordering (OO) to an orbital liquid by enough magnetic fields but did from one type of OO to another OO. Another prominent feature of the ZFC curve is that there is a steep rise in the M-T curve as the temperature increases between 4 and 12 K, and M is nearly invariable between 1.9 and 4 K. According to the intrinsic COAFM phase coexists with FM phase at low temperature, such behaviors could connect with the increase of the FM phase at the expense of the AFM phase fraction, which shows the temperature dependence of the COAFM-FM coexistent phase. In addition, it should be noted that the difference between the values of the magnetization M for the ZFC and FC curves around 110 K might be related to the large magnetostriction presence in this material.[13] The ρ-T curves recorded in the ZFC and FC modes split near $T=130$ K, as M-T curves did. In the low-temperature region ($T<100$ K), ρ-T and M-T curves vary exactly in opposite ways, which is qualitatively consistent with what the double exchange (DE) model predicts. This behavior could be more difficult to understand for $Pr_{1-x}Ca_xMnO_3$ (Ref. 14) with a smaller one-electron bandwidth W of the e_g electrons. In the case, it can be only conjectured that the COAFM state was changed to FM metallic state under the sufficient magnetic field. That is, the CO was melted and the spin was realigned towards FM behavior. And the spin and OO are strongly coupled with each other.[15] As a result, it can be supposed that in this case, magnetic field can affect the $d_{3x^2-r^2}/d_{3y^2-r^2}$-type OO and modulate the spin structure accordingly, and then favor the transformation of AFM phase. Experimentally, it has been observed that the e_g electron preferred to occupy the $d_{x^2-y^2}$ orbital under magnetic field.[16] According to the DE model,[17,18] if the localized t_{2g} spins are considered classically, the transfer integral t of e_g electrons between $Mn^{3+}(t_{2g}{}^3e_g{}^1)$ and $Mn^{4+}(t_{2g}{}^3e_g{}^0)$ ions can be expressed as[19]

$$t = t_0 \cos(\theta/2) \approx t_0\sqrt{(1+m^2)/2}, \qquad (1)$$

where t_0 is the transfer integral in a fully spin-polarized state, m is the normalized magnetization, and θ is the angle between nearest-neighbor spins. The normalized magnetization m depends on temperature according to the following self-consistent equation:[20]

$$m = B_S(\alpha m), \quad \text{with } \alpha = \frac{3S}{1+S}\frac{T_C}{T}, \qquad (2)$$

where

$$B_S(x) = \frac{2S+1}{2S}\mathrm{cth}\left[\frac{2S+1}{2S}x\right] - \frac{1}{2S}\mathrm{cth}\left[\frac{1}{2S}x\right] \qquad (3)$$

denotes the Brillouin function with $S=2-x/2=1.8152$; In order to analyze the effect of temperature on t, we can first fit the m at Curie temperature $T_C=70$ K in terms of Eqs. (2) and (3), in which the T_C value is taken from the FC magnetization result at 6.0 T as displayed in Fig. 2. The fitted m value is quite coincident with the experimental result for the curve $T<T_C$. as shown in the inset of Fig. 2. That is to say, the trend of the curve of t was consistent with the FC magnetization result for $T<T_C$. However, for $T>T_C$, the change of T_N and T_{CO} is not reflected in the fitted curve. Nevertheless, both the theoretically fitted curves and experimental results coincide each other for $T<T_C$, which shows the existence of orbital polaron.[20] This is consistent with the result ρ-T at low temperature as displayed in the inset of Fig. 1, which gives a distinct minimum in the vicinity of 13 K. The resistivity minimum is probably due to the carries localization induced by orbital polarization. Both those reflect the effect of orbital on the transport behaviors, and the effect of spin on the process needs further investigation. Under this case, the appearance of orbital state indicates that the behavior of ρ-T and M-T for PCMO should have an anisotropic characteristic. According to the DE mechanism, the system should show an isotropic behavior by gaining a maximum kinetic energy and has no OO state in the FM metallic state. However, experimental and theoretical results have revealed a complex phase diagram that is certainly beyond the DE ideas, so Jahn-Teller (JT) distortions and orbital order are also needed to understand the physical picture of manganites. Indeed, the $d_{x^2-y^2}$-type orbital ordering was observed in the FM state of 50% hole-doped $Pr_{1/2}Sr_{1/2}MnO_3$ and $Nd_{1/2}Sr_{1/2}MnO_3$.[21] There are theoretical results that simulated the existence of OO in the FM state.[22] So, in the present case, we suggest both the magnetic and electrical transport properties at low-temperature region ($T<100$ K) should have probably the two-dimensional character due to the existence of $d_{x^2-y^2}$ OO state. In addition, it must be noted that the role of spin and orbital on the electrical transport process can be checked at low temperature, since the electrical and magnetic transport properties is correlated with each other. Resistivity versus temperature for different magnetic field should be carried out to investigate detailed the low-temperature resistivity minima as shown in the inset of Fig. 1. The relevant fitted work should be carried out according to $\rho(T)=1/[\sigma(0)+AT^{1/2}]+BT^{9/2}+CT^n$, where $\sigma(0)$ is the residual conductivity and A, B, and C are all constants. $1/\sigma(0)+AT^{1/2}$ denotes electron-electron (e-e) interaction, $BT^{9/2}$ denotes DE contribution, and CT^n denotes additional inelastic contributions. Meanwhile, the resistivity versus T

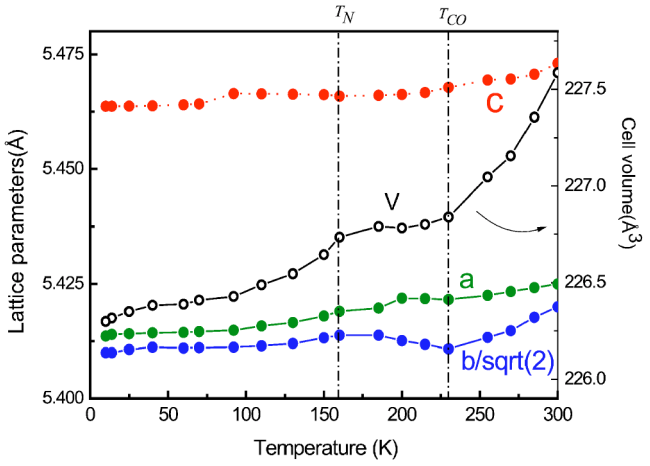

FIG. 3. (Color online) Lattice parameters and unit cell volume as a function of temperature for $Pr_{5/8}Ca_{3/8}MnO_3$ sample.

under variational magnetic field can also study the spin-orbital scattering contribution if the negative magnetoconductance appears.

It is well known that the setting of the CO in manganites can result in significant distortions of the unite cell. This originates from cooperative Jahn-Teller effects and is accompanied by orbital ordering.[23] Recently, the presence of structural anomalies between T_C and T_N, which is related to the development of a strong JT-type distortion with decreasing temperature, have reported by Cox *et al.*[24] In their work, for PCMO, observed phenomena proved that there exist the change of CO and OO as the temperature or the magnetic field vary. In order to study in detail the possible structural distortions as temperature decreases due to CO/OO, we studied the temperature dependence of the lattice parameters and the unit cell volume as shown in Fig. 3. The lattice parameters are calculated based on least square fitting. It can be seen that their behavior is in qualitative agreement with previously published data on similar compounds.[25] The compound has a *Pbnm* orthorhombic perovskite structure,[11] which is evidenced by the decrease of both the lattice parameter b and the unit-cell volume with decreasing temperature near the room temperature. It does be an O′ structure with $b/\sqrt{2}<a<c$ in the range of the measured temperature. To the low temperature behavior, a number of changes on the lattice parameters are correlated to the characteristic of structural and magnetic ordering temperature T_{CO}, T_N, and T_C, respectively. CO/OO are related to the crystal and spin structure, and OO is expected to produce a significant change of the crystal structure and the anisotropy of the spin exchange. As the $d_{3z^2-r^2}$ ordering, for example, the out-of-plane lattice constant c becomes bigger than the in-plane lattice constants a and b, and the exchange interaction along the c axis will be stronger than that within the a-b plane. As Fig. 3 displayed, the lattice parameters display some changes in the region between T_{CO} and T_N, with a drastic increase of b and faintly increase of a after T_{CO}, which indicate the occupancy of the $d_{3x^2-r^2}/d_{3y^2-r^2}$ orbital when $T<230$ K. However, when temperature is below T_N, a and b decrease and c slightly increases, which shows the $d_{3z^2-r^2}$ orbital of e_g electron begins to be occupied. The present observations are in good agreement with the proposed model for the PCMO superstructure by Asaka *et al.*,[11] except that present results show the $d_{3x^2-r^2}/d_{3y^2-r^2}$ orbital should be a long-range ordering when below T_{CO}, though it is not observed by the electron diffraction. Here, the obscure decrease of c should be noticed between T_{CO} and T_C, possibly because the orbital ordering of Mn^{3+} in the a-c plane is mostly compensated for the disordering of the $d_{3z^2-r^2}$ orbital along c axis. That is said that, according to the results of low-temperature XRD, above T_{CO} the e_g electrons randomly distribute in Mn sites, and below T_{CO} there appears $d_{3x^2-r^2}/d_{3y^2-r^2}$ ordering within the a-b plane, while along the c axis $d_{3z^2-r^2}$ is completely disordered. Only when the temperature is below T_N, does the extra Mn^{3+} e_g electron begin to occupy the $d_{3z^2-r^2}$ orbital. In terms of earlier neutron-diffraction result,[26] the extra electron introduced into the structure due to the x concentration changing can modulate the "robustness" of the CO state. Accordingly, the AFM spin structure of the system is also modified, and that it will affect the collapse of the CO domains. In $Pr_{1-x}Ca_xMnO_3$ compounds with $x\sim0.5$, the CO regions is more "harder," and with deviation of x from 0.5, the spin arrangement along the c direction will change and make the CO regions become more "soften." From this point of view, the spin and orbital structure can determine the required critical magnetic field to melt the COAFM phase.

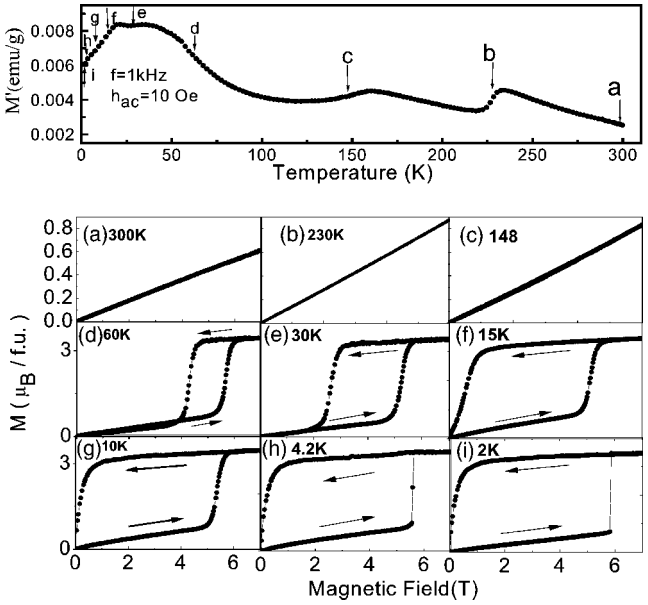

FIG. 4. Results of the ac magnetic susceptibility measurement and the magnetization isotherms at selected temperature to be corresponding to the results of ac susceptibility curve. Which is labled with (a) (300 K), (b) (230 K), (c) (148 K), (d) (60 K), (e) (30 K), (f) (15 K), (g) (10 K), (h) (4.2 K), and (i) (2 K), respectively.

B. Magnetization step and orbital/spin structure

ac magnetic susceptibility measurements have been widely used to characterize magnetic transitions occurring in CMR materials, especially in the PS manganites.[27,28] Figure 4 gives the results of ac magnetic susceptibility and the field dependence of magnetization at selected temperatures in ac

susceptibility curves. For the present measurement, the low ac magnetic field (H_{ac}=10 Oe) is not supposed to affect the magnetic state of the sample. From these results, it can be seen that there are two kinks around 240 and 160 K corresponding to the CO temperature (T_{CO}) and Nèel temperature (T_N), respectively, which is consistent with above electronic and magnetic results. According to the kinks in the M'-T curve, there exist many kinds of magnetic structure as the temperature varies in PCMO. Some representative temperature points are selected which is labeled with (a) (300 K), (b) (230 K), (c) (148 K), (d) (60 K), (e) (30 K), (f) (15 K), (g) (10 K), (h) (4.2 K), and (i) (2 K), respectively, and corresponding M-H curves are measured as shown in Fig. 4(a)–4(i). For each measurement, the sample was cooled under zero-field from room temperature to the selected temperature, M-H curves were measured in a cycle sweeping mode ($0\rightarrow 7.0\ \mathrm{T}\rightarrow 0\rightarrow -7.0\ \mathrm{T}\rightarrow 0$) with a sweeping rate of 60.0 Oe per s. It can be seen that the M at 300, 230, and 148 K increases linearly in proportion to the applied field until 7.0 T. On the whole, the slope of M-H curve is related to the magnetization value at selected temperature point as shown in the ac susceptibility curve. There is a little decrease of the M-H curve slope for 148 K comparing with 230 K. It should be noticed that temperature point (b), T=230 K, lies below the CO transition T_{CO} near and point (c), T=148 K, below the AFM transition T_N about. From increasing slope for M-H curve, it shows that magnetic order is stronger in CO phase than in AFM state. This indicates that the change of magnetization under magnetic field should be related to the orbital polaron.[20] For the M-H curve below 60 K, an initial magnetization increases linearly with H, which indicates the AFM phase domains at the low field. At a critical magnetic field H, a field-induced step occurs, associating with the transition of COAFM phase fraction to FM state. The magnetization reaches almost a saturation moment of $3.45\mu_B$/f.u. at 7.0 T, which is consistent with the expected value for $Pr_{5/8}Ca_{3/8}MnO_3$ in theory and this highly magnetized state can be regarded as a fully spin-polarized phase. As we have seen in Figs. 4(d), 4(e), 4(f), and 4(g), the transition from AFM to FM state shows a gradual character. However, this behavior changes dramatically below 4.2 K as shown in Figs. 4(h) and 4(i), which shows an abrupt step near H_c =5.5 and 5.8 T for T=4.2 and 2 K, respectively. Their width are smaller than 1×10^{-4} T. In the frame of martensitic scenario, the strains created at the AFM/FM interfaces tend to block the development of the magnetic energy. And when the applied magnetic filed is sufficient to overcome the stress energy, the magnetization will appear a sudden increase. This is consistent with the appearance of abrupt M-H steps below 4.2 K. While for the gentle step above 10 K, according to the phase separation model, it seems to suggest a process during which the critical magnetic field drives this transition in different parts of the sample. Why they behave different transformation process for the temperature below 4.2 K and above 10 K? Both models did not give satisfactory explanation. Actually, the sharp step appeared below 4.2 K and fairly weak critical fields (only ~6.0 T at 2 K), as shown in the isothermal magnetization curves in Fig. 4, would not be understood only based on simply competition between the FM and COAFM. If the steps originate from equally strong and competing AFM and FM exchange interaction, spin fluctuations would inevitably be enhanced in the boundary of FM clusters and COAFM, and smear the transition. In addition, both models give only a mesoscopic picture to the magnetization transitions because of the mesoscopic phase coexistence of COAFM and FM fractions. In terms of the result of Figs. 1 and 2, we have displayed the contribution of orbital state to the transport process, which shows that applied magnetic field not only acts on the spin of AFM phase fraction, but also can induce the variety of orbital. The anisotropic AFM ordering of spins in the sample as shown in Fig. 5 is one of the manifestation of the coupling between spins and orbitals.[23,26,29] Moreover, the critical field driving the steps is remarkably small (Fig. 4), which is consistent with mean-field and numerical relaxation analysis[14] and further indicates the steps are closely related to the spin and charge structure. All these findings thus favor a drastic change of the microscopic spin orientation at the M-H steps. Indeed, using the numerical simulation results according to coupling between spin and orbital degree of freedom,[15] Koshibae *et al.* find a charasteristic magnetization process of manganites. Based on the data above, we conjecture a scenario in which the occurrence of M-H steps is due to a microscopic spin reorientation of the AFM phase due to the change of OO with the magnetic field. As for the steps of M-H above 10 K, which becomes a gentle slop, it is the effect of thermal fluctuations that smears the transition. The suppose is accordant with the model of spin and orbital coupling of Koshibae *et al.*, which think that the recovering of spin ordering depends strongly on the state of orbital in the e_g state of Mn ions. In other words, the spin moment is accompanied with the change of the orbital structure and finally results in a magnetization process of manganites, which shows only a typical phenomenon of the stabilization of specific spin values.

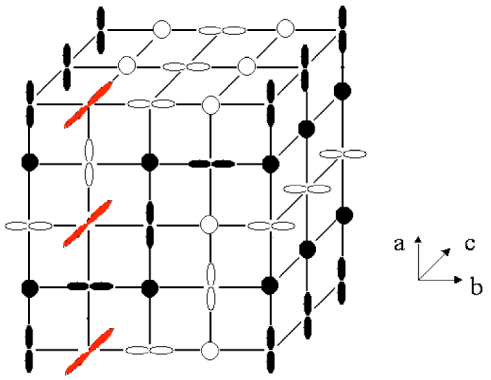

FIG. 5. (Color online) The charge/orbital ordering and magnetic structure of $Pr_{5/8}Ca_{3/8}MnO_3$ at low temperature.

For a $Pr_{1-x}Ca_xMnO_3$ system, the effective hopping of e_g, i.e., the kinetic energy of e_g electron can be given as

$$\tilde{H}_t = t_0 \sum_{\langle ij\rangle\sigma\mu\nu} t_{ij}^{\mu\nu}\tilde{c}_{i\mu\sigma}^{+}\tilde{c}_{j\nu\sigma}^{+} + \mathrm{H.c.}, \qquad (4)$$

where $\tilde{c}_{i\mu\sigma}(\tilde{c}_{i\mu\sigma}^{+})$ denotes the annihilation (creation) operator with spin σ in the μ orbital on site i with the constraint. $t_{ij}^{\mu\nu}$

is a hopping integral between μ orbital on site i and ν orbital on site j. When an external magnetic field is applied in the z direction, the Zeeman term can be introduced,

$$H_Z = -2\mu_B H \sum_i (S_i^{zt_{2g}} + S_i^z). \quad (5)$$

For PCMO, in the COAFM phase, the Hund coupling together with kinetic energy as shown in Eq. (4), can induce an effective ferromagnetic interaction between the sites occupied and unoccupied by an e_g electron. The spin state can be easily modified by the magnetic field due to the suppression of AFM interaction $J_{t_{2g}}$ by the effective FM interaction. Therefore the ordering of spin and orbital of ground state is determined self-consistently. Finally, when magnetic field is applied, the spin was modulated by orbital and the step appears, which is consistent with the results in Fig. 4.

The structure of PCMO and the correlation of CO/OO with spin mode as the applied magnetic field varies can be illustrated by the charge/orbital ordering and magnetic structure of PCMO at low temperature as shown in Fig. 5. Just contrary to the "$x=1/2$ plus defects" scenario due to x away from 0.5, there is no defect to be constructed into the specific charge arrangements. Because, for $Pr_{5/8}Ca_{3/8}MnO_3$, the ratio of Mn^{3+} to Mn^{4+} in the sublattice is 5:3 according to the chemical composition, except that the alternation of $(3x^2-r^2)$ and $(3y^2-r^2)$ orbital appears in the a-b planes, and the extra e_g electrons occupy $3d_{z^2-r^2}$ orbital on the Mn^{4+} sublattice which is along the c direction instead of parallel to the a-b layers.[24] This charge/orbital pattern is consistent with our XRD results. It should be noted that the Coulomb interaction in this charge state is lowest and plays an important role in the observed CO phase.[9,30] The magnetic structure at low temperature as shown in Fig. 5 is commonly described as the pseudo-CE type for $Pr_{5/8}Ca_{3/8}MnO_3$.[14,26,31] The spin ordering arrangement is a single FM zigzag chain with alternating Mn^{3+} and Mn^{4+} ions along the corner sites. However, all the neighboring chains will exhibit ferromagnetic ordering except that the $(3z^2-r^2)$ orbital is occupied. Along the c axis, the neighboring a-b planes stack with no change and the AFM Mn-O layers are ferromagnetic coupled. The observation will essentially mean that an electron passes a corner site of the zigzag chain and acquires a phase that depends on the orbital through it passes. This can lead to an effective dimerization that splits the bands and open a gap at the Fermi surface.[32] Maybe, the gap can determine the value of critical magnetic field H_C of the step occurrence.

The effective ferromagnetic interaction depends on which orbital is occupied by an e_g electron. So, the different orbital case in the ground state will make the spin structure have different change with increasing magnetic field. According to the CO/OO and spin structure in Fig. 5, the magnitude of the effective FM interaction (J_{34}) for $Pr_{5/8}Ca_{3/8}MnO_3$ is nearly zero, which is an average result based on different orbital occupied. So the relative spin structure can change into complete FM state at a certain magnetic field without intermediate phase transition. This should be the reason that only one step occurs. It must be pointed out that the complete FM state after steps should be an orbital liquid state with random

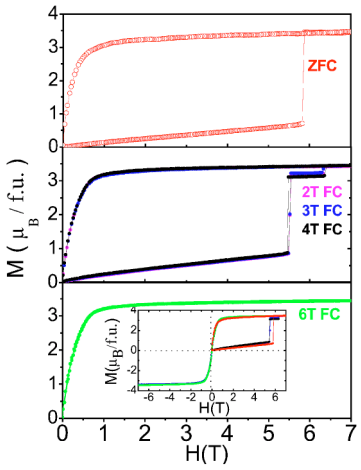

FIG. 6. (Color online) M-H curves at $T=2$ K after cooling in different positive fields.

orbital disorder. In fact, in terms of this explanation, the M-H step should behave sharply. However, it can be found from Fig. 4 that between 60 and 10 K, with the increase of magnetic field, the step shows a gentle slop, while it dose not display a sharp step transition as it does below 4.2 K. From the numerical results about the coupling between the spin and orbital degrees of freedom,[15] it can be concluded that the magnetization process is not scaled by only $J_{t_{2g}}$, but is determined by the balance of magnitude between $J_{t_{2g}}$ and the effective FM interaction caused by t_0 and the Hund coupling. For the experimental results between 60 and 10 K in Fig. 4, this magnetization process can be attributed to the ratio of $J_{t_{2g}}/t_0$. Here, $J_{t_{2g}}$ is temperature dependent. As the temperature increases, the effective FM interaction is suppressed due to the thermal fluctuation. Therefore, $J_{t_{2g}}/t_0$ is larger above 10 K than that below 4.2 K, so the step becomes more gentle slop when temperature is above 10 K. The results can also be understood according to the change of t as temperature decreases. From inset of Fig. 2, we can find t becomes bigger after $T<T_C$, so this can possibly explain why the M-H steps are easy to appear under only several T. According to the orbital polaron theory,[20] the fluctuation rate of orbital is $\propto xt$: the stronger the orbital fluctuates, the more its stabilization is unfavorable. Then, the large fluctuation rate of orbital will make easily the corresponding spin orientation, i.e., it will need less energy to cause the occurrence of steps below 60 K. As for the difference above 10 K and below 4.2 K, it is because the thermal fluctuation affects the fluctuation rate of orbital above 10 K and the COAFM-FM step is not sharp.

It is more interesting that two sharp steps appear for PCMO system in the different FC conditions at $T=2.0$ K as shown in Fig. 6. All these FC magnetization curves are obtained with field cooled from 300 K, and after stabilization at the measurement temperature 2 K, the field was reduced to zero, and then M-H was measured in a field sweeping mode $(0\rightarrow 7.0\ \mathrm{T}\rightarrow 0\rightarrow -7.0\ \mathrm{T}\rightarrow 0)$. Surprisingly, the field cooled M-H in magnetic field 2.0, 3.0, and 4.0 T are nearly the same, and there are all two jumps occurred near the same critical fields. Only when the sample is cooled in a sufficient high magnetic field 6.0 T, does the M-H curve display an

almost fully ferromagnetic state and eliminate the steps. But the twofold step is difficult to be accounted for merely by the martensitic mechanism. In the frame of martensitic model,[6] the occurrence of multisteps on *M-H* curves is such that: When the field value is high enough to locally overcome the stress constraints, it will trigger a sudden motion of FM/COAFM interfaces in a part of the sample and then induce a abrupt increase of the magnetization. Along this process, the magnetic energy decrease and the stress energy increase, which can lead the system to be frozen in another metastable balance state. Then, the overall transition may appear successive steps on the *M-H* curves. However, according to the result of low-temperature XRD as displayed in Fig. 3, the low-temperature CO phase is long-range ordered in the sample. Though the XRD experiment shows no trace of FM phase in the sample it should be understandable in terms of a long-range-ordered characteristic.[33] Since there exists a balance between long-range-ordered FM and COAFM phases in the sample, the magnetic energy is only needed to overcome one type of stress energy created at the COAFM/FM interfaces. Because applied magnetic field should be simultaneously acts on the whole sample uniform. Then it will be only one step appears with magnetic field increasing. The appearance of similar twofold steps at different FC conditions is difficult to understand according to the simple martensitic transition. The present FC twofold step phenomena prove the existence of the spin quantum phase transition due to the interplay of spin and orbital orderings, which should reflect an intrinsic property in the strong correlation manganite systems. FC may stabilize certain types of spin structure and accordingly the orbital structure also changes with the spin structure. So the effective FM interaction J_{34} will have a certain value. That is to say, FC can modulate the orbital ordering state of $Pr_{5/8}Ca_{3/8}MnO_3$, and when the *M-H* begins to be measured under magnetic field, the orbitals can gain energy through the J_{34} term. Thus, as the magnetic field increases, a certain type of spin and orbital state will be stabilized in the intermediate process. In Fig. 6, it shows that the FC curves at 2.0, 3.0, and 4.0 T are similar, which indicate that they should stabilize the same type of spin structure during the cooling process. Then, with increasing magnetic field, the state with certain magnetization value (here is about 3.2 μ_B/f.u.) appears. The corresponding orbital structure also changes with the spin structure. We suppose that there is possible presence of $d_{x^2-y^2}$ orbital ordering at the intermediate spin state just on the second step boundary, which increases the transfer integral t of the e_g electrons and the FM interaction. The character of the preferred e_g state under magnetic field is similar to that of $La_{1-x}Sr_xMnO_3$.[16] Meanwhile, it should be noted that the coupling constant of spin and orbital is anisotropic due to the dependence on hopping integral t_{ij}^{ab}. If we chose the orbital basis as a, $b \in \{|3z^2-r^2\rangle, |x^2-y^2\rangle\}$, the transfer matrices will be denoted as

$$t_{x/y}^{ab} = t\begin{pmatrix} 1/4 & \mp\sqrt{3}/4 \\ \mp\sqrt{3}/4 & 3/4 \end{pmatrix} \text{ and } t_z^{ab} = t\begin{pmatrix} 1 & 0 \\ 0 & 0 \end{pmatrix}, \qquad (6)$$

which indicate that the orientation at a given bond can determine the transfer amplitude, and consequently affect the spin orientation of the system. With further increasing magnetic field, the perfect FM state with orbital degeneracy appears. Therefore, since the ordering of spin and orbital is determined self-consistently, the quantum phase transition of magnetization is history dependent on the spin and orbital structure. According to our explanations, it must be emphasized that the value of critical field, which drives the COAFM-FM transition, should be given by the spin and orbital structure, i.e., the robustness of the CO phase in the PS system. Therefore, they must be well reproducible and independent of the relative fraction of two phases. The property will be easy to be proved using additional thermal treatments to a ceramic sample since the phase separation can be controlled by the grain boundaries,[34] the chemical pressure, and oxygen-isotope composition.[1]

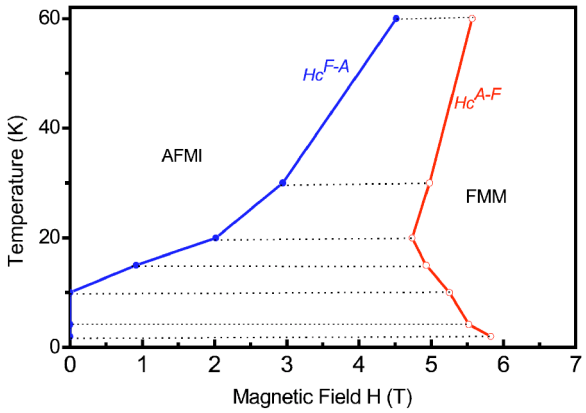

FIG. 7. (Color online) Magnetic phase diagram for $Pr_{5/8}Ca_{3/8}MnO_3$ against an external critical magnetic field. Open and closed circles represent the $H_C^{A\text{-}F}$ and $H_C^{F\text{-}A}$, respectively. AFMI and FMM stand for antiferromagnetic insulator and ferromagnetic metal, respectively.

In addition to the field-induced magnetization steps, the experimental data in Fig. 4 also convey the character of the thermal effect, for which the *M-H* curve depended strongly on temperature. For the *M-H* curve below 60 K, the critical magnetic field of the transition of COAFM to FM state, i.e., the critical field induced the appearance of step, can be defined as $H_C^{A\text{-}F}$. For the measurement process from 7.0 to 0 T, the *M-H* at 30 and 60 K remains in FM behavior initially and then appears a FM-AFM transition at critical magnetic field, which can be defined as $H_C^{F\text{-}A}$. For the *M-H* curves measured below ~10 K, however, a typical long-range ferromagnetic behavior appears. From the experimental data, we give the magnetic transition phase diagram at low temperature in Fig. 7. Here, a hatched area shows a hysteretic region, which is the characteristics of first order phase transition and displays a bistable region where the COAFM and FM state can coexist. Meanwhile, the present phenomena also show that magnetic field can induce the appearance of PS state in the system. The hysteretic region depends critically on temperature and becomes broader as temperature decreases, which is due to the suppression of the effect of thermal fluctuation on the phase transition boundary. And this is thought to be a generic feature of the first order phase transition at low temperature.[35] From Fig. 7, we can also see

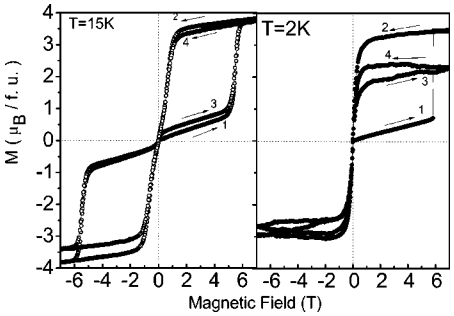

FIG. 8. *M-H* curves were measured by two successive sweeping cycling of magnetic field at 15 and 2 K, respectively.

that both the critical magnetic field $H_C^{A\text{-}F}$ and $H_C^{F\text{-}A}$ are function of temperature below 60 K. The critical field to destroy the CO state enhances with the increase of temperature in the low-temperature region, which is similar to the relative experiment results for $x=0.5$ and is inconsistent with $x=0.35$ and 0.40.[36] It is also clear that $H_C^{A\text{-}F}$ in $Pr_{5/8}Ca_{3/8}MnO_3$ below and above ~20 K are different, even though the applied magnetic field at or above H_c is required to overcome the energy barrier between AFM and FM under isothermal conditions. The energy barrier determines the value of critical magnetic field at a finite temperature. Below ~20 K, $H_C^{A\text{-}F}$ increases with decreasing temperature because the thermal fluctuations of the localized magnetic moments and/or elasticity of the lattice in the AFM state are reduced, thus enhancing the negative exchange interaction. The increased negative exchange interaction raises the energy barrier between AFM and FM state, and the larger $H_C^{A\text{-}F}$ is needed to accomplish the transition. Since the formation of the FM is accompanied by a contract of the crystal structure,[24] this results in the dominating positive exchange interaction and thermal fluctuation at low temperature is not strong enough to destroy the FM state in $Pr_{5/8}Ca_{3/8}MnO_3$. Therefore, the AFM-FM transition is irreversible below ~20 K. On the other hand, the free energy difference between AFM and FM state also increases with temperature above 20 K, and so does the critical magnetic field. This increase may be associated with the thermal expansion of the $Pr_{5/8}Ca_{3/8}MnO_3$ crystal lattice, for which the small changes in interatomic distances may have a pronounced effect on the free energies of the AFM and FM states.[37] However, $H_C^{A\text{-}F}$ increases all along with the temperature increasing above ~20 K, which is likely caused by the increased thermal fluctuation and/or thermal expansion of the lattice and then increases the energy barrier of the AFM and FM state in the $Pr_{5/8}Ca_{3/8}MnO_3$ system.

C. Metastable magnetic order and history-dependent magnetization

In order to study the low-temperature properties in more detail, we performed the measurements of *M-H* by two successive sweeping cycling of magnetic field at 15 K and 2 K, respectively. The relevant results are given in Fig. 8. Samples were zero-field cooled before a magnetic field was increased according to the cycling of two continuous $0\rightarrow 7.0\ T\rightarrow 0\rightarrow -7.0\ T\rightarrow 0$ sweeping process. From Fig. 8, it can be found that for the *M-H* curve measured at $T=15$ K there exists a nearly rectangular loop and the virgin curve itself lies outside of this loop. Here, no hysteresis is observed for both. Compared to the curve at 15 K, the loop of virgin curve at 2 K is sharper, and the curve of the second cycle displays FM state even at the beginning measurement of the second cycling. This phenomenon shows that the FM part is history dependent and has also the character of memory effect. Only by heating the sample above 160 K, could the sample recover its original state, which shows that it is highly temperature sensitive. On the other hand, at low temperature the resistivity decreases to 10^{-4} magnitudes on an applied field of 6.0 T as shown in Fig. 1. The resistivity and magnetization of ZFC and FC processes are very different (see Fig. 2). All these results indicate the existence of the metastable magnetic ordering, which is possibly caused by a field-induced change in the orbital occupancy of e_g electron.[38,39] Meanwhile, a large magnetostriction appears in the magnetization process due to the magnetic field.[15] The mechanism of magnetostriction is originated from the interchange coupling of magnetic moment of atoms. In terms of the charge, orbital and spin ordering structure at low temperature for $Pr_{5/8}Ca_{3/8}MnO_3$ as shown in Fig. 5, the magnetostriction under the applied field may improve the orbital overlap within the plane and enhance the probability of the charge transfer. Actually, the wave function of $d_{x^2-y^2}$ stretches along the *x* axis and *y* axis, then the distance between 3*d* and O^{2-} along the same axis becomes larger than that along *z* axis, which will induce the lower free energy and the system is more stable. These phenomena mean the possible presence of $d_{x^2-y^2}$ orbital ordering and thus increase the transfer integral *t* of the e_g electrons and increase the FM interaction. The characteristics above are consistent with the steps of *M-H* due to the interplay of spin and orbital. The appearance of second curve within the virgin curve is because of the history of spin and orbital structure. In this sense, the present history-dependent magnetization is related to the orbital structure. A situation with the spins standing perpendicular on the orbitals rather than pointing in the orbital plane seems to be energetically preferred.

IV. CONCLUSIONS

In order to clarify the physical mechanism of magnetization step in strong correlation manganites with phase separation, the $Pr_{5/8}Ca_{3/8}MnO_3$ single crystal was successfully grown by the optical floating-zone method and investigated systematically on the structural, magnetic, and transport properties. Theoretically, the destruction of the orbital ordering by an external field gives rise to the structural phase transition and the recovering of the DE, which promotes the polarization of the t_{2g} spins. In the present case, the field-induced magnetostriction occurs and indicates orbital occupancy of the e_g electron of the Mn^{3+} change with the magnetic filed. And then this orbital occupancy causes the occurrence of the *M-H* step and the history-dependent magnetization effect. The step becomes ultrasharp below 4.2 K.

In the FC conditions, the two sharp steps appear at $T=2$ K, which shows a possible existence of spin quantum transition. The results proved that all the magnetization steps and history-dependent magnetization effects were related to the interplay of spin and orbital degrees of freedom, indicating the presence of a field-induced change in the orbital occupancy of the e_g electron of the Mn^{3+}, which shows the possible appearance of $d_{x^2-y^2}$ orbital ordering. On the other hand, the directional dependence of the spin and OO correlations was clearly observed in the FC *M-H* measurement, which further makes sure the fact that the spin fluctuations are driven by the specific $d_{x^2-y^2}$-type orbital ordering in the intermediate step process.

ACKNOWLEDGMENTS

This work is supported by the National Foundation of National Science of China (Grant No. 10274049), The Key-project of the Science & Technology Committee of Shanghai Municipality (Grant No. 04JC14039), Down Project of the Education Committee of Shanghai Municipality (Grant No. 03SG35) and the Key Subject of Shanghai Educational Committee.

*Email address: jczhang@staff.shu.edu.cn

[1] M. Uehara, S. Mori, C. H. Chen, and S.-W. Cheong, Nature (London) **399**, 560 (1999).
[2] A. Moreo, S. Yunoki, and E. Dagotto, Science **283**, 2034 (1999).
[3] S. Hébert, V. Hardy, A. Maignan, R. Mahendiran, M. Hervieu, C. Martin, and B. Raveau, J. Solid State Chem. **165**, 6 (2002); Solid State Commun. **122**, 335 (2002).
[4] A. Maignan, S. Hébert, V. Hardy, C. Martin, M. Hervieu, and B. Raveau, J. Phys.: Condens. Matter **14**, 11 809 (2002).
[5] R. Mahendiran, A. Maignan, S. Hébert, C. Martin, M. Hervieu, B. Raveau, J. F. Mitchell, and P. Schiffer, Phys. Rev. Lett. **89**, 286602 (2002).
[6] V. Hardy, S. Hébert, A. Maignan, C. Martin, M. Hervieu, and B. Raveau, J. Magn. Magn. Mater. **264**, 183 (2003).
[7] M. Tokunaga, N. Miura, Y. Tomioka, and Y. Tokura, Phys. Rev. B **57**, 5259 (1998).
[8] V. Hardy, S. Majumdar, S. Crowe, M. R. Lees, D. M. Paul, L. Herve, A. Maignan, S. Hebert, C. Martin, C. Yaicle, M. Hervieu, and B. Raveau, Phys. Rev. B **69**, 020407(R) (2004).
[9] S. Yamada, T. Arima, H. Ikeda, and K. Takita, J. Phys. Soc. Jpn. **69**, 1278 (2000).
[10] Y. Tomioka, A. Asamitsu, H. Kuwahara, Y. Moritomo, and Y. Tokura, Phys. Rev. B **53**, R1689 (1996).
[11] T. Asaka, S. Yamada, S. Tsutsumi, C. Tsuruta, K. Kimoto, T. Arima, and Y. Matsui, Phys. Rev. Lett. **88**, 097201 (2002).
[12] E. Pollert, S. Krupićka, and E. Kuzmićová, J. Phys. Chem. Solids **43**, 1137 (1982).
[13] G. Xiao, E. J. McNiff, G. Q. Gong, A. Gupta, C. L. Canedy, and J. Z. Sun, Phys. Rev. B **54**, 6073 (1996).
[14] Takashi Hotta and Elbio Dagotto, Phys. Rev. B **61**, R11 879 (2000).
[15] Koshibae, Y. Kawamura, J. Inoue, and S. Maekawa, J. Phys. Soc. Jpn. **10**, 2985 (1997).
[16] H. Kawano-Furukawa, R. Kajimoto, H. Yoshizawa, Y. Tomioka, H. Kuwahara, and Y. Tokura, Phys. Rev. Lett. **78**, 4253 (1997).
[17] P. W. Anderson and H. Hasegawa, Phys. Rev. **100**, 675 (1955).
[18] P.-G. de Gennes, Phys. Rev. **118**, 141 (1960).
[19] A. J. Millis, B. I. Shraiman, and R. Mueller, Phys. Rev. Lett. **77**, 175 (1996).
[20] R. Kilian and G. Khaliullin, Phys. Rev. B **60**, 13 458 (1999).
[21] H. Kawano-Furukawa, R. Kajimoto, H. Yoshizawa, Y. Tomioka, H. Kuwahara, and Y. Tokura, Phys. Rev. B **67**, 174422 (2003).
[22] S. Yunoki, A. Moreo, and E. Dagotto, Phys. Rev. Lett. **81**, 5612 (1998).
[23] J. B. Goodenough, Phys. Rev. **100**, 564 (1955).
[24] D. E. Cox, P. G. Radaelli, M. Marezio, and S. W. Cheong, Phys. Rev. B **57**, 3305 (1998).
[25] P. Dai, J. Zhang, H. A. Mook, S. H. Liou, P. A. Dowben, and E. W. Plummer, Phys. Rev. B **54**, R3694 (1996).
[26] Z. Jirák, S. Krupicka, Z. Simsa, M. Dlouha, and Z. Vratislav, J. Magn. Magn. Mater. **53**, 153 (1985).
[27] J. H. Zhao, X. Z. Zhou, A. Peles, S. H. Ge, H. P. Kunkel, and G. Williams, Phys. Rev. B **59**, 8391 (1999).
[28] P. Vanderbemden, B. Vertruyen, A. Rulmont, R. Cloots, G. Dhalenne, and M. Ausloos, Phys. Rev. B **68**, 224418 (2003).
[29] I. Solovyev, N. Hamada, and K. Terakura, Phys. Rev. Lett. **76**, 4825 (1996).
[30] Y. Okimoto, Y. Tomioka, Y. Onose, Y. Otsuka, and Y. Tokura, Phys. Rev. B **59**, 7401 (1999).
[31] C. Frontera, J. L. Garcia-Munoz, A. Llobet, M. Respaud, J. M. Broto, J. S. Lord, and A. Planes, Phys. Rev. B **62**, 3381 (2000).
[32] J. van den Brink, G. Khaliullin, and D. Khomskii, Phys. Rev. Lett. **83**, 5118 (1999).
[33] G. R. Blake, L. Chapon, P. G. Radaelli, D. N. Argyriou, M. J. Gutmann, and J. F. Mitchell, Phys. Rev. B **66**, 144412 (2002).
[34] P. Levy, F. Parisi, G. Polla, D. Vega, G. Leyva, H. Lanza, R. S. Freitas, and L. Ghivelder, Phys. Rev. B **62**, 6437 (2000).
[35] H. Kuwahara, Y. Tomioka, A. Asamitsu, Y. Moritomo, and Y. Tokura, Science **270**, 961 (1995).
[36] K. Nakamura, T. Arima, A. Nakazawa, Y. Wakabayashi, and Y. Murakami, Phys. Rev. B **60**, 2425 (1997).
[37] A. Asamitsu, Y. Tomioka, H. Kuwahara, and Y. Tokura, Nature (London) **388**, 50 (1997).
[38] I. Gordon, P. Wagner, V. V. Moshchalkov, Y. Bruynseraede, M. Apostu, R. Suryanarayanan, and A. Revcolevschi, Phys. Rev. B **64**, 092408 (2001).
[39] Y. Konishi, T. Kimura, M. Izumi, M. Kawasaki, and Y. Tokura, Appl. Phys. Lett. **73**, 3004 (1998).